Potassium Ion Controlled Switching of Intra- to Intermolecular Electron Transfer in Crown Ether Appended Free-Base Porphyrin−Fullerene Donor−Acceptor Systems

Francis D'Souza,*,† Raghu Chitta,† Suresh Gadde,† Melvin E. Zandler,† Amy L. McCarty,† Atula S. D. Sandanayaka,‡ Yasuyaki Araki,‡ and Osamu Ito*,‡

Department of Chemistry, Wichita State University, 1845 Fairmount, Wichita, Kansas 67260-0051, and Institute of Multidisciplinary Research for Advanced Materials, Tohoku University, Katahira, Sendai, 980-8577, Japan

Received: September 17, 2005; In Final Form: December 13, 2005

Photoinduced electron transfer in intramolecularly interacting free-base porphyrin bearing one or four 18-crown-6 ether units at different positions of the porphyrin macrocycle periphery and pristine fullerene was investigated in polar benzonitrile and nonpolar *o*-dichlorobenzene and toluene solvents. Owing to the presence of two modes of binding, stable dyads were obtained in which the binding constants, *K*, were found to range between 4.2×10^3 and 10.4×10^3 M^{-1} from fluorescence quenching data depending upon the location and number of crown ether entities on the porphyrin macrocycle and the solvent. Computational studies using the B3LYP/3-21G(*) method were employed to arrive at the geometry and electronic structure of the intramolecular dyads. The energetics of the redox states of the dyads were established from cyclic voltammetric studies. Under the intramolecular conditions, both the steady-state and time-resolved emission studies revealed efficient quenching of the singlet excited free-base porphyrin in these dyads, and the measured rates of charge separation, k_{CS}, were found to be in the 10^8-10^9 s^{-1} range. Nanosecond transient absorption studies were performed to characterize the electron-transfer products and to evaluate the charge-recombination rates. Shifting of the electron-transfer pathway from the intra- to intermolecular route was achieved by complexing potassium ions to the crown ether cavity(ies) in benzonitrile. This cation complexation weakened the intramolecular interactions between fullerene and the crown ether appended free-base porphyrin supramolecules, and under these conditions, intermolecular type interactions were mainly observed. Reversible inter- to intramolecular electron transfer was also accomplished by extracting the potassium ions of the complex with the addition of 18-crown-6. The present study nicely demonstrates the application of supramolecular methodology to control the excited-state electron-transfer path in donor−acceptor dyads.

Introduction

Control of electron/energy-transfer pathways in donor−acceptor systems by utilizing novel supramolecular concepts (self-assembled multicomponent systems) not only is important to enhance our knowledge on the mechanistic details of complex biological electron-transfer processes,[1] but is also useful toward constructing molecular electronic devices[2] and sensors[3] and in light energy harvesting.[4−8] Control over the mechanism and the rate of electron/energy-transfer processes using the supramolecular approach, both spatially and energetically, are important factors. Although the energetic characteristics of these systems can be manipulated relatively easily, spatial control, in terms of direction, mechanism, and rate of energy/electron transfer, can be achieved only when the interactions between the donor and acceptor entities, that is, the orbital nature of both ground and excited electronic states, are understood. Toward this, the construction and study of photoinduced electron/energy transfer in donor−acceptor systems are important and several books and reviews have appeared covering different aspects of this area of research.[4−8] Among the donor−acceptor systems, porphyrin−fullerene systems are one of the widely studied classes of compounds due to their rich photo- and redox chemistry.[9−17] Systems linked both covalently and noncovalently by hydrogen bonds, by van der Waals forces, by electrostatic interactions, by $\pi-\pi$ stacking, or by metal−ligand coordination systems all have been elegantly designed and studied. Fullerenes require small reorganization energy in electron-transfer reactions, owing to their spherical geometry.[18] Consequently, in donor−acceptor systems, fullerenes accelerate forward electron transfer (k_{CS}) and slow backward electron transfer (k_{CR}) resulting in the formation of long-lived charge-separated states. This property of fullerene has been found useful in the design of molecular devices.[10f]

In the case of porphyrin−fullerene donor−acceptor supramolecular systems, both intra- and intermolecular type interactions play an important role in governing the photochemical reaction pathways.[9−17] Control over the molecular structure and topology has often been achieved by utilizing multiple modes of binding.[10,17] For this, both the porphyrin and fullerene entities were functionalized possessing one or more binding (self-assembling) sites. Intramolecular $\pi-\pi$ type interactions between porphyrin and fullerene,[14] and between crown ether and fullerene,[19] are well-known in the literature. These interactions, although weak in solution, are subject of interest during the past few years.[14,19] One way to improve such weak interactions and further utilize the resulting stable complexes to probe light induced electron transfer is by covalently linking the porphyrin

* To whom correspondence should be addressed. E-mail: Francis.DSouza@wichita.edu; E-mail: ito@tagen.tohoku.ac.jp.
† Wichita State University.
‡ Tohoku University.

10.1021/jp055284u CCC: $33.50
Published on Web 03/16/2006

SCHEME 1

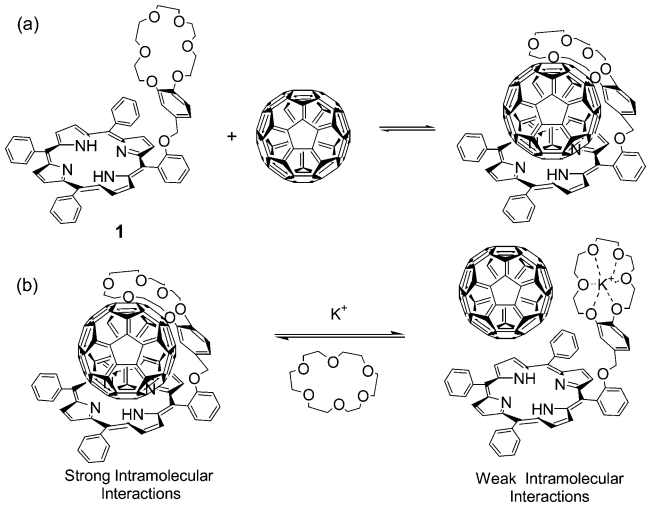

(a) Structure of benzo-18-crown-6 appended free-base porphyrin, **1**, and it's binding to C_{60}. (b) Potassium ion induced switching of intra- to intermolecular association (forward reaction) and 18-crown-6 induced reversible switching of the inter- to intramolecular process (backward reaction).

SCHEME 2: Structures of the 18-crown-6 Appended Free-base Porphyrins, 2 and 4, and Probable Structures of the C_{60} Complexes

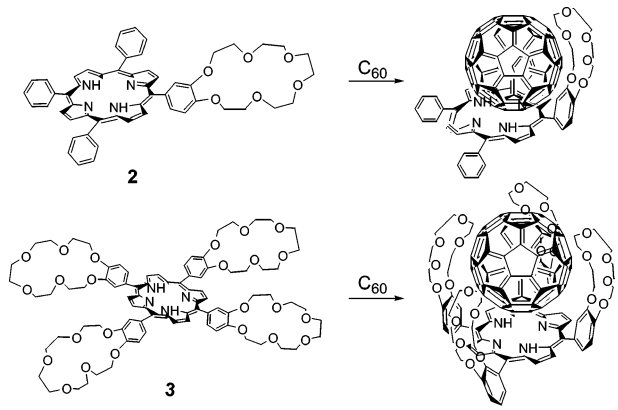

and crown ether entities in such a way that both the functionalities contribute toward binding the fullerene in a cooperative fashion, thereby increasing the stability of the resulting complex. This has been achieved in the present study where stable complexes are formed between crown ether appended porphyrins and pristine fullerene (Schemes 1a and 2). As a consequence, efficient intramolecular photoinduced electron transfer has been achieved in these self-assembled dyads in both polar, benzonitrile and nonpolar, *o*-dichlorobenzene, and toluene solvents.

Furthermore, switching of intra- to intermolecular electron transfer in the studied donor−acceptor dyads has been achieved by complexing potassium ions to the crown ether cavity. Because of the resulting planarity and decreased nucleophilicity[20] of the potassium−crown ether complex, no strong intramolecular interactions with fullerene were observed, as shown in Scheme 1b (forward reaction). Under these solution conditions, only intermolecular bimolecular photochemical events from triplet excited porphyrin to the fullerene are observed. Interestingly, when the potassium ions were extracted by the addition of 18-crown-6 to the solution (reverse reaction in Scheme 1b), switching of the inter- to intramolecular process was accomplished. As demonstrated in the present study (i) the binding of both the crown ether and porphyrin moieties of the donor entity to the acceptor, pristine fullerene, in a cooperative fashion, leading to intramolecular photochemical electron transfer and (ii) reversible switching of the electron-transfer path from an intra- to intermolecular upon potassium cation complexation into the crown ether voids are important factors since it not only demonstrates the supramolecular cooperative binding to form stable complexes but also reveals switching of the excited-state reaction mechanism, for the first time to our knowledge, in donor−acceptor systems.

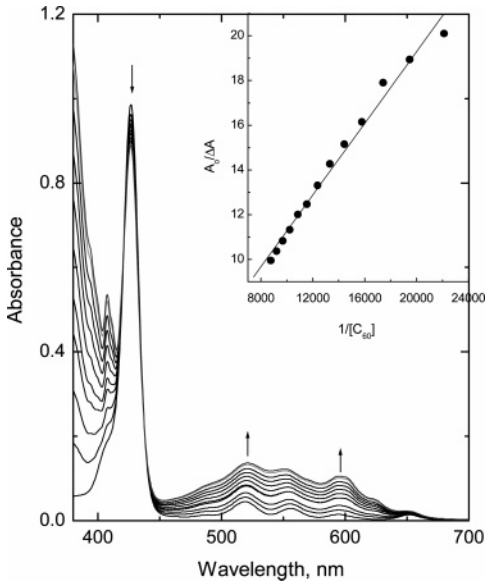

Figure 1. UV−vis spectral changes observed during the titration of **3** (1.7 μM) with C_{60} (3.2 μM each addition) in toluene. The figure inset shows the Benesi−Hildebrand plot constructed for measuring the binding constant.

Results and Discussion

UV−vis Spectral Studies and Ground-State Interactions. The optical absorption spectra of the free-base porphyrin macrocycle with the benzo-18-crown-6 appended at different *meso*-positions were found to be similar to that of pristine *meso*-tetraphenylporphyrin, H_2TPP.[19] That is, they exhibited an intense Soret band around 420 nm and four less intense visible bands in the 500−700 nm region, respectively. No apparent absorption band in the wavelength region covering 350−700 nm corresponding to the crown ether entities was observed. The addition of pristine fullerene to a solution containing either of porphyrins **1**, **2**, or **3** revealed spectral changes accompanied by two or more isosbestic points. Typical spectral changes are shown in Figure 1 for porphyrin **3** in the presence of increasing amounts of pristine fullerene in toluene. Similar changes were observed in *o*-dichlorobenzene and benzonitrile. The Soret band revealed a decrease in intensity with one to two isosbestic points, which is typical of $\pi-\pi$ interacting porphyrin donor−acceptor systems. The observed isosbestic points indicate the presence of a one-equilibrium process in solution. No new absorption band in the near-IR region covering the 650−1000 nm range was observed corresponding to the charge-transfer interactions,[17] probably due to the extended free-base porphyrin absorption bands (up to 700 nm) into this wavelength region. Job's plots of continuous variation also confirmed the 1:1 molecular stoichiometry of the supramolecular complexes. Using the absorption data, the binding constants (*K*) for the formation of self-assembled dyads were obtained by constructing Benesi−Hildebrand plots[21] (Figure 1 inset). The *K* values thus obtained ranged (2.2−5.6) $\times$ 10^3 M^{-1} as listed in Table 1. It may be mentioned here that

TABLE 1: Binding Constants for the Self-assembled Crown Ether Appended Free-base Porphyrin−Fullerene Conjugates in Different Solvents

		K, M^{-1} [b]	
dyad[a]	solvent	UV−vis	fluorescence
H_2TPP:C_{60}	PhCN	$<10^3$ [c]	1.1×10^3
	DCB	$<10^3$ [c]	1.1×10^3
	toluene	$<10^3$ [c]	1.2×10^3
1:C_{60}	PhCN	2.4×10^3	6.6×10^3
	DCB	2.9×10^3	8.3×10^3
	toluene	5.6×10^3	10.4×10^3
2:C_{60}	PhCN	2.2×10^3	4.2×10^3
	DCB	2.7×10^3	4.7×10^3
	toluene	4.7×10^3	7.4×10^3
3:C_{60}	PhCN	2.3×10^3	5.6×10^3
	DCB	2.8×10^3	6.9×10^3
	toluene	4.9×10^3	7.9×10^3

[a] See Schemes 1 and 2 for the structure of the porphyrins. [b] Calculated from the Benesi−Hildebrand plots (error = ±10%). [c] Estimated after employing correction for fullerene absorption at the monitoring wavelength.

the nonnegligible absorbance of C_{60} at the Soret band position of porphyrins compensated the apparent decrease of the Soret band absorbance causing a slight deviation of the linear Benesi−Hildebrand plots. This leads to an underestimation of the K values to some extent (vide infra).

In a control experiment, H_2TPP, that is, free-base porphyrin bearing no crown ether entities was titrated with C_{60}. A slight decrease in the Soret band intensity was observed. When the increase of the absorbance of the added C_{60} is taken into account, the estimated K values were found to be far less than $\sim 1 \times 10^3$ M^{-1}. These results clearly demonstrate the importance of multiple modes of binding to achieve higher stability of supramolecular complexes.

Complexing the 18-crown-6 ether entity(ies) of the porphyrin(s) by the addition of 10 equiv potassium tetrakis(4-chlorophenyl)borate decreased the intramolecular interactions with C_{60} considerably. That is, only marginal changes with no clear isosbestic points were observed suggesting weak or an absence of intra−supramolecular interactions between the free-base porphyrin and fullerene (See Figure S1 in Supporting Information for spectral details). This could be rationalized based on the decreased nucleophilicity and planar structure of the potassium ion complexed 18-crown-6[20] entity which would not favor binding of the electron deficient spherical fullerene. Under these conditions, as depicted in Scheme 1b, the free-base porphyrin−fullerene interactions were not strong enough to reveal significant spectral changes.

Steady-State Fluorescence Studies. The singlet excited-state quenching of crown ether appended free-base porphyrins by functionalized fullerenes was investigated to obtain the binding constants of the self-assembled dyads and the overall fluorescence intensity quenching behavior with respect to differently assembled free-base porphyrin−fullerene dyads. The porphyrins were excited at a wavelength corresponding to the isosbestic point observed at the higher wavelength side of the Soret band (~430 nm). The fluorescence behavior of the crown ether appended free-base porphyrins was found to be similar to that of the free-base porphyrins with two fluorescence bands around 652 and 720 nm. The addition of C_{60} to a solution containing either of the porphyrins, **1**, **2,** or **3**, revealed fluorescence quenching in all of the investigated solvents. Representative fluorescence changes of **1** upon the increasing addition of C_{60} in benzonitrile are shown in Figure 2. Through the use of the fluorescence data, the binding constants (K) for the formation

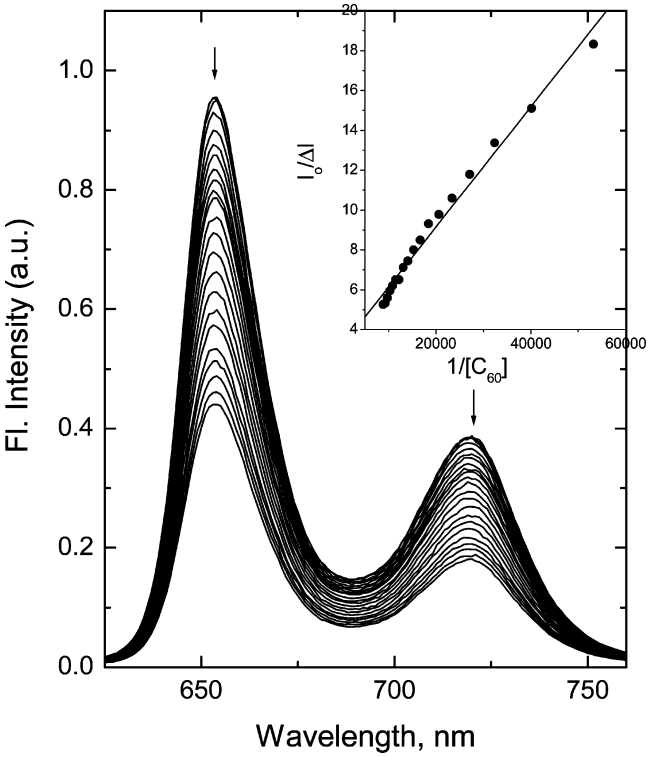

Figure 2. Fluorescence spectral changes observed upon increasing addition of C_{60} (2.8 μM each addition) to a solution of **1** (2.5 μM) in benzonitrile. The sample was excited at the isosbestic point of 432.6 nm. The figure inset shows the Benesi−Hildebrand plot (monitored at 655 nm) constructed for measuring the binding constant in benzonitrile (I_0 is the fluorescence intensity in the absence of **1** and ΔI is the changes of fluorescence intensity upon addition of C_{60}).

of self-assembled dyads were obtained by constructing Benesi−Hildebrand plots[21] (Figure 2 inset), and the data are listed in Table 1. It may be mentioned here that the K values evaluated from fluorescence data are much more reliable since these values are obtained after eliminating the added C_{60} concentrations with excitation at the isosbestic point.

An examination of the binding data in Table 1 reveals the following: (i) The K values for the crown ether bound free-base porphyrins, **1**−**3**, interacting with C_{60} were much higher than that observed for pristine porphyrin−fullerene interactions. (ii) The K values obtained from the fluorescence data were generally more reliable compared with that obtained from the optical absorption spectral data, since our attempt to subtract the fullerene absorption at the monitoring absorption wavelength was not fully successful. (iii) The K values followed the trend: **H_2TPP:C_{60}** ≪ **2:C_{60}** < **3:C_{60}** < **1:C_{60}** for a given solvent and were generally higher in nonpolar solvents. The trend in the K values with different porphyrins (**2:C_{60}** < **1:C_{60}**) could be attributed to the proximity effects caused by the crown ether entity at a different location of the porphyrin macrocycle. The trend in the K values with a different number of crown ethers (**2:C_{60}** < **3:C_{60}**) could be attributed to better cooperative binding effects caused by the crown ether entities of the porphyrin macrocycle as shown in Scheme 1b. The smaller K values in polar benzonitrile could also be due to the limited solubility and subsequent aggregation of C_{60}.

The Stern−Volmer plots for the fluorescence intensity quenching of the crown ether appended free-base porphyrins by C_{60} were also examined. The observed Stern−Volmer constants, K_{SV} values, were found to range between 7×10^2 and 6×10^3 M^{-1}. It may be mentioned here that, when pristine

TABLE 2: B3LYP/3-21G(*) Optimized Geometric Parameters of the Self-assembled Crown Ether Appended Free-base Porphyrin−Fullerene Conjugates

dyad[a]	Ct-to-Ct[a] distance, Å	Ed-to-Ed[b] distance, Å	association energy, kcal/mol[c]
1:C$_{60}$	8.20	4.38	−10.26
2:C$_{60}$	6.58	3.15	−5.66
3:C$_{60}$	6.46	3.12	−12.19

[a] Distance between the center of the free-base porphyrin to the center of the C_{60} spheroid. [b] Distance from the nearest porphyrin π-ring atom to the fullerene spheroid carbon. [c] At the B3LYP/3-21G(*) level.

H_2TPP was utilized, the quenching was found to be much smaller ($\sim 10^2$ M^{-1}) than that observed for the crown ether appended porphyrin in the studied solvents. Upon employing the excited-state lifetime of free-base porphyrin to be 9.6 ns, the bimolecular fluorescence quenching rate constants were evaluated to be (7.2×10^{10} to 6.2×10^{11} M^{-1} s^{-1}), which are up to 2 orders of magnitude higher than that expected for diffusion controlled bimolecular quenching processes in the studied solvents ($\sim 5.0 \times 10^9$ M^{-1} s^{-1}) suggesting that the intra−supramolecular processes are responsible for the fluorescence quenching. The tendency of increasing K_{SV} values was in good agreement with those evaluated K values.

As predicted from the absorption spectral studies, recovery of the fluorescence intensity was observed upon the addition of K^+ to a solution of crown ether appended porphyrin−C_{60} dyad (see Figure S2 in the Supporting Information for spectral details). That is, the binding of K^+ to the crown ether entity-(ies) weakened the porphyrin−fullerene intramolecular interactions as shown in Scheme 1b. However, the recovered emission intensity was nearly 60% of the original intensity of the porphyrin (monitored at the 720 nm emission band) suggesting the occurrence of weak intra- or intermolecular processes under the present solution conditions (vide infra).

DFT B3LYP/3-21G(*) Computational Studies. The geometry and electronic structure of the crown ether appended free-base porphyrin−fullerene dyads were calculated by using the B3LYP/3-21G(*) method.[22] The space-filling model structures of the self-assembled **1:C$_{60}$**, **2:C$_{60}$**, and **3:C$_{60}$** dyads are shown in Figure 3, and the key geometric parameters are given in Table 2. For geometry optimization, the starting porphyrin and fullerene entities were initially optimized on a Born−Oppenheimer potential energy surface and then allowed to interact.

The optimized structures of dyads **1:C$_{60}$**, **2:C$_{60}$**, and **3:C$_{60}$** revealed the expected complex formation due to fullerene interacting with both the porphyrin and crown ether entities. In the structure of **1:C$_{60}$**, the crown ether entity was pawed a little over the C_{60} spheroid and the porphyrin ring was puckered slightly. In the case of **2:C$_{60}$** and **3:C$_{60}$**, no significant distortion of the porphyrin ring was noticed; however, an initial slight bending of the 18-crown-6 entity(ies) was needed to facilitate the interaction with the fullerene that was positioned centrally on the porphyrin π-ring. As shown in parts b and c of Figure 3, the dyads optimized in these geometries, although stable structures in other molecular orientations may be possible. Because of the different position of the crown ether moieties on the porphyrin macrocycle, the topologies of the dyads were slightly different, as shown in Figure 3. The center-to-center distance and edge-to-edge distances between the free-base porphyrin and fullerene entities were 1−2 Å larger for **1:C$_{60}$** compared to the respective distances of **2:C$_{60}$** and **3:C$_{60}$** (Table 2). Fullerene was found to be symmetrically positioned above the porphyrin macrocycle in the case of **2:C$_{60}$** and **3:C$_{60}$**. The edge-to-edge distances between the closest porphyrin π-ring atom to the fullerene spheroid carbon atom were found be slightly smaller than the van der Waals distances. The edge-to-edge distance between the fullerene spheroid carbon and crown ether oxygen in all of the structures varied between 2.96 and 3.16 Å suggesting intramolecular type interactions between these entities. These results suggest $\pi-\pi$ type interactions between the crown ether appended free-base porphyrin and fullerene entities participate in the binding process, in addition to the $n-\pi$ type interaction between the fullerene and crown ether entities.

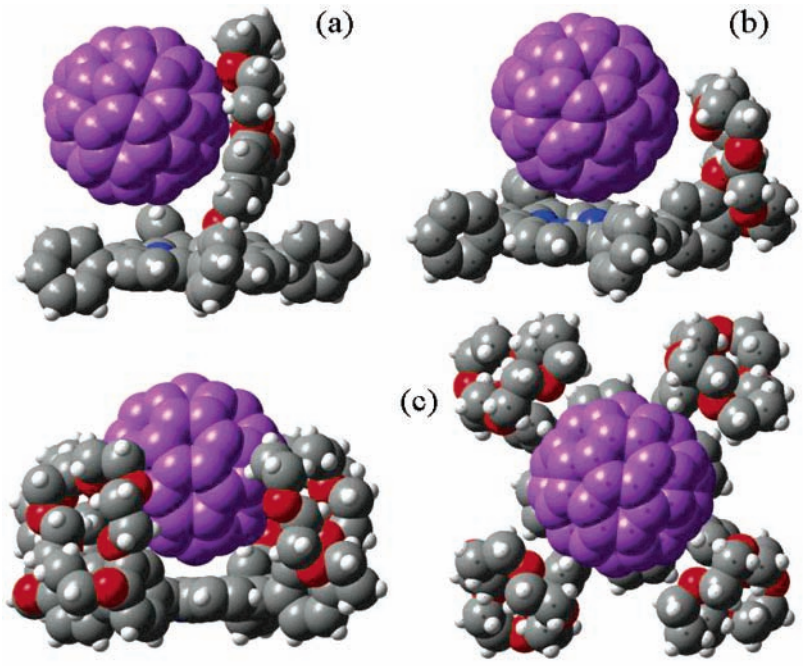

Figure 3. DFT B3LYP/3-21G(*) optimized space-filling model structures of (a) **1:C$_{60}$**, (b) **2:C$_{60}$**, and (c) **3:C$_{60}$** (in two orientations): C, gray (C_{60}, magenta); O, red; N, blue; H, white.

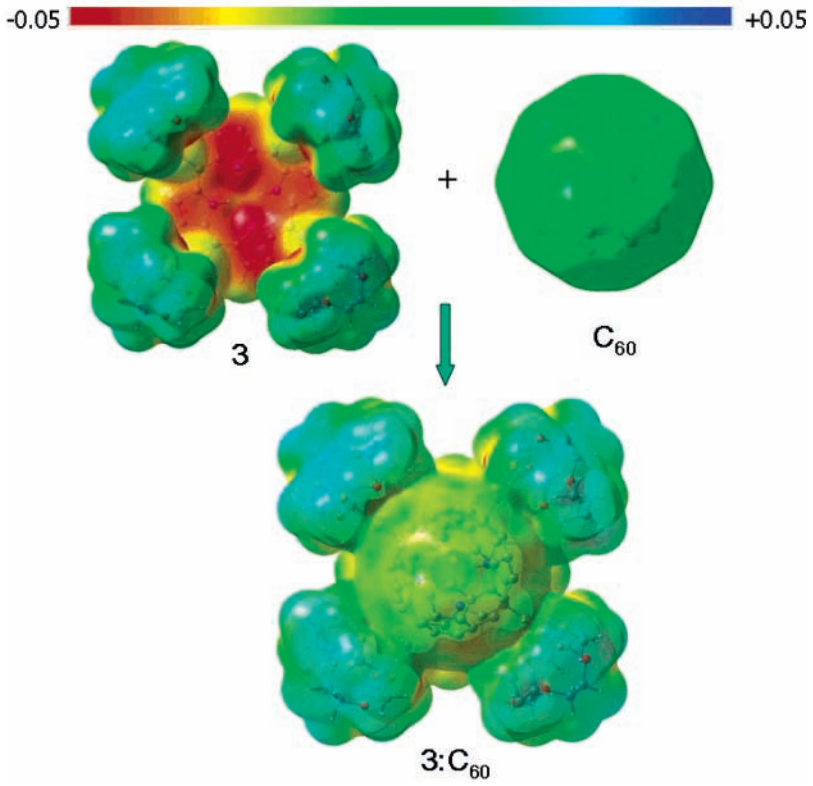

Figure 4. Molecular electrostatic potential maps of **3**, C_{60}, and the **3**:C_{60} supramolecular complex for the B3LYP/3-21G(*) optimized structures. The bar on the top shows the scale (magnitude) of the electrostatic potential.

The stable structures of **1:C_{60}**, **2:C_{60}**, and **3:C_{60}** clearly demonstrate the usefulness of employing both porphyrin and crown ether moieties in the self-assembly process. The association energy was estimated from the difference between the total energy of the supramolecular complex and the sum of the individual host and guest entities separated from the optimized structure (single-point calculation). These association energies at the B3LYP/3-21G(*) level were found to range between −5.7 and −12.2 kcal/mol (see Table 2). These negative association energies suggest stable supramolecular complex formation, and the trend in the magnitude of these values track the *K* values in Table 1. However, these complexes are much weaker compared to the earlier reported metal−axial coordination (∼20−30 kcal/mol)[16d] or crown ether−ammonium cation complexation (100−125 kcal/mol)[17b] energies calculated at the B3LYP/3-21G(*) level.

Further, the molecular electrostatic potential maps (MEPs),[22] all at a potential scale range of −0.05 (red) to +0.05 (blue), were generated for **3**, C_{60}, and **3**:C_{60} to visualize the electrostatic interactions (Figure 4). The maps for **3** and C_{60} were created by simply pulling apart the **3**:C_{60} complex without optimization of the moieties, that is, no relaxation. The MEP for **3** showed negative electrostatic potential (shown in red) on the porphyrin ring (mostly located on the nitrogen atoms) and on the crown ether oxygen sites. The MEP for C_{60} was blue-green, indicating positive electrostatic potential. Interestingly, in the supramolecular complex, **3**:C_{60}, the original blue-green color of the separated C_{60} changed to green and the deep red color of porphyrin changed to red-yellow (see the scale on top of Figure 4) indicating charge-transfer interactions as one of the major binding forces. The ground-state charge transfer, estimated by summing all of the Mulliken charges, was about 0.03 e from the porphyrin moiety to the fullerene moiety. In all of the studied dyads, the frontier highest occupied molecular orbital (HOMO) was found to be located on the free-base porphyrin entity and the frontier lowest unoccupied molecular orbital (LUMO) was found to be located on the fullerene entity (not shown). No HOMO or LUMO contribution was observed on the appended crown ether entities. These results suggest that the charge-separated state in electron-transfer reactions of the supramolecular dyads is $H_2P^{\bullet+}$:$C_{60}^{\bullet-}$.

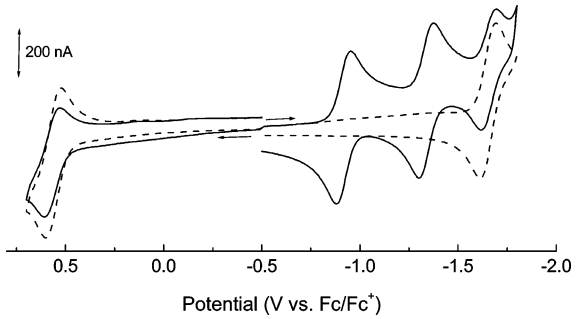

Figure 5. Cyclic voltammograms of **1** (∼0.5 mM, dashed line) and **1** + **C_{60}** (∼0.5 mM, solid line) in benzonitrile, 0.1 M (n-Bu)$_4$NClO$_4$. Scan rate = 100 mV/s.

Electrochemical Studies. Cyclic voltammetric studies were performed to evaluate the redox potentials of the dyads and to establish the associated free-energy changes for electron-transfer reactions in the studied solvents. The crown ether appended free-base porphyrins, **1**−**3**, revealed a one-electron oxidation process corresponding to the formation of $H_2P^{\bullet+}$ and one-electron reduction corresponding to the formation of $H_2P^{\bullet-}$, respectively. Extending the potential window beyond the first oxidation process resulted in a large anodic wave, perhaps due to the oxidation of the appended crown ether entities.[23] As shown in Figure 5, the first oxidation and the first reduction processes were found to be fully reversible for **1** in the investigated solvent. Upon forming the dyad **1:C_{60}** by the addition of 1 equiv

TABLE 3: Electrochemical Half-wave Redox Potentials ($E_{1/2}$ vs Fc/Fc^+) for the Crown Ether Appended Free-base Porphyrin−Fullerene Dyads in the Presence of 0.1 M $(n\text{-}Bu)_4NClO_4$ in Benzonitrile (PhCN) or *o*-Dichlorobenzene (DCB)[a]

compound	solvent	$H_2P^{0/\bullet+}$/ V	$C_{60}^{0/\bullet-}$/ V	$H_2P^{0/-}$/ V	$-\Delta G_{CS}$[b]/ eV	$-\Delta G_{CR}$[b]/ eV
1	PhCN	0.56		−1.65		
	DCB	0.50		−1.77		
1:C_{60}[c]	PhCN	0.56	−0.92	−1.65	0.53	1.41
	DCB	0.51	−1.08	−1.78	0.42[d]	1.52[d]
	toluene				0.07[d]	1.87[d]
2	PhCN	0.52		−1.65		
	DCB	0.50		−1.76		
2:C_{60}[c]	PhCN	0.52	−0.92	−1.65	0.59	1.35
	DCB	0.50	−1.08	−1.77	0.51[d]	1.43[d]
	toluene				0.29[d]	1.65[d]
3	PhCN	0.53		−1.66		
	DCB	0.50		−1.77		
3:C_{60}	PhCN	0.53	−0.93	−1.66	0.68	1.26
	DCB	0.50	−1.08	−1.78	0.50[d]	1.44[d]
	toluene				0.29[d]	1.65[d]

[a] Driving forces for the forward (ΔG_{CS}) and reverse (ΔG_{CR}) electron transfer in PhCN, DCB, and toluene. [b] See text for details. [c] Obtained by the equimolar addition of porphyrin and fullerene. [d] Values of ΔG_{CS} and ΔG_{CR} in toluene and DCB were evaluated from the equation $\Delta G_S = (e^2/(4\pi\epsilon_0))[(1/(2R_+) + 1/(2R_-) - 1/R_{(Ct-Ct)})/\epsilon_S - (1/(2R_+) + 1/(2R_-))/\epsilon_R]$,[24] where ϵ_S and ϵ_R refer to the solvent dielectric constant for photophysical measurements and electrochemical measurements (PhCN).

of C_{60}, fully reversible first and second reduction processes of C_{60} were found in the −0.7 to −1.4 V potential region. The half-wave potentials were found to be not significantly different from C_{60} (<5 mV change) in the absence of any added porphyrin (Table 3). The oxidation potential of **1** also experienced a cathodic shift of less than 10 mV.

The driving forces for charge recombination ($-\Delta G_{CR}$) and charge separation ($-\Delta G_{CS}$) were calculated according to eqs 1 and 2 using the electrochemical redox data[24]

$$-\Delta G_{CR} = E_{ox} - E_{red} - \Delta Gs \quad (1)$$

$$-\Delta G_{CS} = E_{0,0} - (-\Delta G_{CR}) \quad (2)$$

where E_{ox} is the first oxidation potential of the porphyrin ($H_2P^{0/\bullet+}$), E_{red} is the first reduction potential of the fullerene ($C_{60}^{0/\bullet-}$), and $\Delta E_{0,0}$ is the energy of the 0−0 transition between the lowest excited state and the ground state of the free-base porphyrin evaluated from the fluorescence peaks being 1.94 eV. ΔG_S refers to the static energy, calculated by using the "dielectric continuum model"[24] according to eq 3. The symbols

$$\Delta G_S = e^2/(4\pi\epsilon_0\epsilon_S R_{Ct-Ct}) \quad (3)$$

ϵ_0 and ϵ_S represent vacuum permittivity and dielectric constant of the solvents, respectively. The values of center-to-center distance, R_{Ct-Ct}, were based on the computed structures given in Table 2.

The calculated free-energy changes in Table 3 reveal that the charge-separation process from the singlet excited H_2P to fullerene in these dyads is exothermic, dependent on solvent polarity, and is almost the same as the reorganization energy.[11d,18a] These results predict the occurrence of rapid charge separation in these supramolecular dyads since the ΔG_{CS} values are on the top region of the Marcus parabola.[4,18] On the other hand, the charge recombination in $H_2P^{\bullet+}$:$C_{60}^{\bullet-}$ of the supramolecular complexes predicts the slower process since the highly exothermic ΔG_{CR} values lie on the inverted region of the Marcus parabola.[4,18]

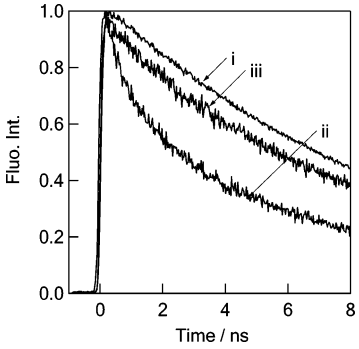

Figure 6. Fluorescence decays at 630−750 nm in benzonitrile for (i) **2** (0.10 mM), (ii) **2** (0.10 mM) + C_{60} (0.12 mM), and (iii) **2** (0.10 mM) + C_{60} (0.12 mM) + K^+ (>10 mM).

TABLE 4: Fluorescence Lifetime (τ_f), Charge-separation Rate Constant (k_{CS}^S), Charge-separation Quantum Yield (Φ_{CS}^S), Charge-recombination Rate Constant (k_{CR}), and Lifetime of the Radical Ion Pair (τ_{RIP}) for the Investigated Crown Ether Appended Free-base Porphyrin−C_{60} Dyads

complex	solvent	τ_f, ns (fraction)	k_{CS}^S, s^{-1}	Φ_{CS}^S	k_{CR}, s^{-1}	τ_{RIP}, ns
1:C_{60}	PhCN	0.68 (59%) 6.78 (41%)	1.4×10^9	0.93	8.2×10^7	13
	DCB	1.80 (60%) 6.60 (40%)	5.0×10^8	0.81	1.7×10^8	6
	TN	2.03 (35%) 7.80 (65%)	3.8×10^8	0.77	8.1×10^7	12
2:C_{60}	PhCN	0.44 (47%) 6.03 (53%)	2.2×10^9	0.95	8.8×10^7	12
	DCB	2.14 (44%) 7.80 (56%)	3.6×10^8	0.76	7.7×10^7	13
	TN	2.40 (41%) 7.60 (59%)	3.0×10^8	0.73	9.1×10^7	11
3:C_{60}	PhCN[a]	0.49 (25%) 7.70 (75%)	1.9×10^9	0.95	1.2×10^8	8
	DCB	1.88 (65%) 6.88 (35%)	4.0×10^8	0.79	1.1×10^8	9
	TN	1.90 (42%) 7.80 (58%)	4.1×10^8	0.79	8.3×10^7	12

[a] The fluorescence time profiles are shown in the Supporting Information.

Picosecond Fluorescence Lifetime Studies. The time-resolved fluorescence studies of the self-assembled dyads tracked those of steady-state measurements. Figures 6 shows the fluorescence decay profiles of the crown ether appended porphyrins, **2**, in the absence and presence of C_{60}. The lifetimes ($(\tau_f)_{ref}$) of the singlet excited crown ether appended free-base porphyrins were found to be 9.60, 9.45, and 9.12 ns for **1**, **2**, and **3**, respectively, and all of them revealed monoexponential decay (curve i in Figure 6). The appended crown ether moieties had a small quenching effect on the lifetime of the singlet excited free-base porphyrin. The addition of 1.0 equiv of C_{60} to the crown ether appended porphyrins caused rapid fluorescence decay in addition to the slow decaying tail as shown in curve ii in Figure 6 (see Figure S3 for data on the **3:C_{60}** dyad). The porphyrin fluorescence time profile showing rapid decay in the dyads could be fitted satisfactorily by a biexponential decay curve, the lifetimes (τ_f) of which are summarized in Table 4. In nonpolar toluene, a similar shortening of the fluorescence lifetimes of the H_2P moiety was also observed; from the slightly negative ΔG_{CS} in toluene, the observed shortening of fluorescence lifetimes in all of the solvents can be attributed to charge separation. The short lifetimes of H_2P ($(\tau_f)_{complex}$) are predominantly due to charge separation within the supramolecular dyads, whereas the long lifetime components are attributed to the

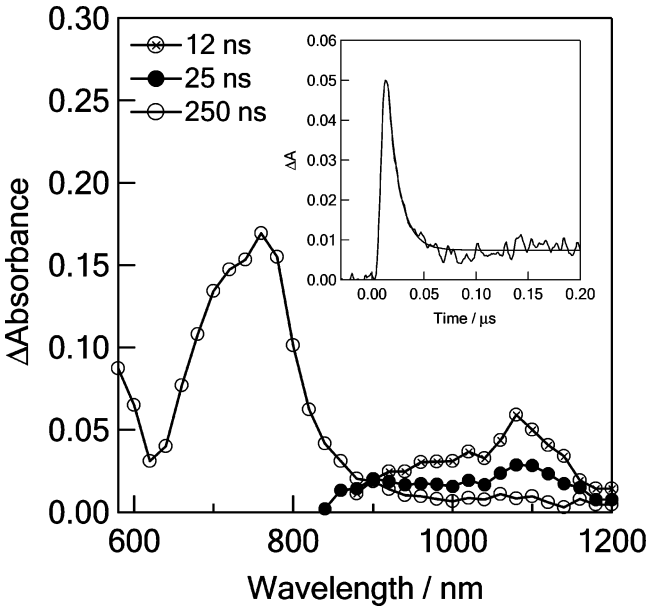

Figure 7. Nanosecond transient absorption spectra of **2** (0.10 mM) in the presence of C_{60} (0.12 mM) after the 532 nm laser irradiation in benzonitrile. The figure inset shows the time profiles of the fullerene anion radicals monitored at 1080 nm for **2:C$_{60}$**.

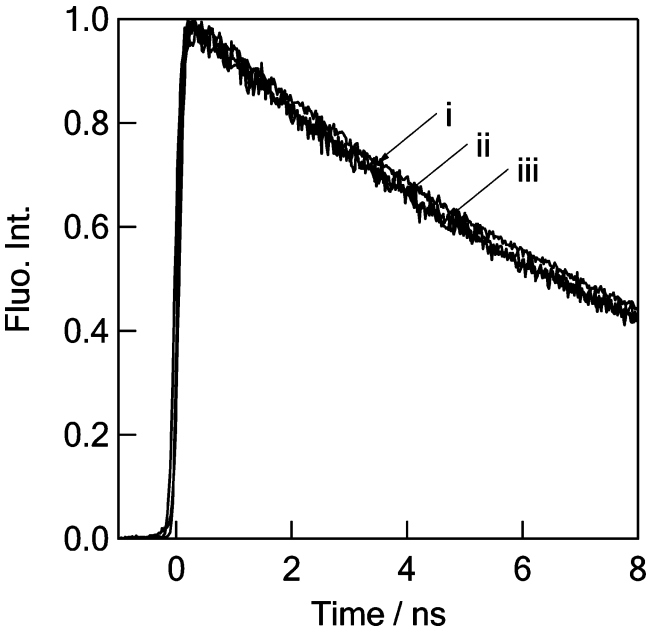

Figure 8. Fluorescence decays for (i) **2** (0.10 mM), (ii) **2** (0.10 mM) + K^+ (1.00 mM), and (iii) **2** (0.10 mM) + K^+ (1.00 mM) + C_{60} (0.12 mM).

uncomplexed free-base porphyrin emission. As shown in Table 4, the fraction of the complexed dyads evaluated from the fraction of fast quenching is in the range of 35−65%, which was slightly larger than the complex fractions (25−40%) calculated from the *K* values (fluorescence data in Table 1).

The charge-separated rates (k_{CS}^S) and quantum yields (Φ_{CS}^S) were evaluated from the short τ_f components according to eqs 4 and 5, a procedure commonly adopted for an intramolecular electron-transfer process.[10]

$$k_{CS}^{S} = (1/\tau_f)_{complex} - (1/\tau_f)_{ref} \quad (4)$$

$$\Phi_{CS}^{S} = [(1/\tau_f)_{complex} - (1/\tau_f)_{ref}]/(1/\tau_f)_{complex} \quad (5)$$

As listed in Table 4, higher values of k_{CS}^S and Φ_{CS}^S were obtained for all of the dyads indicating the occurrence of efficient charge separation irrespective of the location of the crown ether entity on the porphyrin macrocycle. Importantly, the k_{CS} values tracked the solvent polarity, that is, with increasing the solvent polarity, an increase in the k_{CS}^S and Φ_{CS}^S values was observed. Furthermore, nanosecond transient absorption spectral studies were also performed to characterize the electron-transfer products.

Nanosecond Transient Absorption Studies. The nanosecond transient spectra recorded after 532 nm laser irradiation (pulse width = 6 ns) of the crown ether appended free-base porphyrins, **1**−**3**, revealed absorption peaks at 620 and 800 nm corresponding to the excited triplet state of free-base porphyrin.[16] Fullerene, C_{60}, showed a band around 740 nm corresponding to its excited triplet state.[25] Figure 7 shows the transient absorption spectra of **2:C$_{60}$** (fraction of dyad = 30%) at different time intervals. In these spectra, in addition to the peaks corresponding to the triplet excited free-base porphyrin and fullerene, a peak around 1080 nm corresponding to the formation of the fullerene anion radical was observed immediately after the laser irradiation. Similar spectral features were observed for the studied **1:C$_{60}$** dyad (fraction = 36%) and **3:C$_{60}$** dyad (fraction = 33%) (see Figure S4 for results on the **3:C$_{60}$** dyad). These spectral features provide experimental proof for the assigned charge-separation fluorescence quenching mechanism.

As shown in the inset of Figure 7, the time profile of the $C_{60}^{\bullet-}$ transient band at 1080 nm revealed a quick rise and decay typical of intramolecular charge separation via the excited singlet states. The slow decay part after 50 ns may be attributed to the tail of the triplet slow decay. To calculate the rate of charge recombination, k_{CR}, the initial decay of the fullerene anion radical peak at 1080 nm until 50 ns was monitored. The time profiles of these peaks for all of the studied dyads followed first-order decay kinetics once again suggesting the occurrence of an intramolecular charge-recombination process of the radical ion pair. The lifetimes of the radial ion pairs, τ_{RIP}, evaluated as the reciprocal of k_{CR} are listed in Table 3. The τ_{RIP} values of about 10 ns suggest close proximity between the radical ions in the supramolecular dyads. Collectively, the steady-state and time-resolved emissions, as well as the transient absorption studies, indicate the occurrence of intramolecular charge separation and charge recombination in the investigated supramolecular dyads as shown in Schemes 1a and 2.

Intra- to Intermolecular Electron Transfer upon the Addition of Potassium Ions into the Crown Ether Voids of the Supramolecular Complex. The photochemical behavior of crown ether appended free-base porphyrin interacting with C_{60} was investigated in the presence of potassium cations to probe the effect on the stability of supramolecules. As discussed earlier, the steady-state absorption and fluorescence studies suggested occurrence of little or no intramolecular interactions when the crown ether voids were complexed with potassium cations. This is supported by the fluorescence time profiles observed when C_{60} was added after the addition of potassium cations to crown ether appended free-base porphyrin as shown in Figure 8. No acceleration of the fluorescence decay was observed for **2**:K^+ upon the addition of C_{60}. A similar behavior was observed for **1** and **3**. As pointed out earlier, the potassium−crown ether complex is expected not to interact with the fullerene due to its planar structure[20] and decreased nucleophilicity. Thus, the inclusion of the potassium into the crown ether moiety increases the planarity, decreasing the binding ability of C_{60}.

TABLE 5: Fluorescence Lifetime (τ_f), Charge-separation Rate Constant (k_{CS}^S), and Charge-separation Quantum Yield (Φ_{CS}^S) for the Investigated Crown Ether Appended Free-base Porphyrin−C_{60} Dyads in the Presence of K^+ and 18-crown-6 Ether in Benzonitrile

complex	K^+, mM	18-crown-6, mM	τ_f, ns	k_{CS}^S, s^{-1}	Φ_{CS}^S
1:C_{60}	0	0	0.68 (59%) 6.78 (41%)	1.4×10^9	0.93
	1.0	0	0.86 (35%) 6.90 (65%)	1.0×10^9	0.90
	1.0	>10	0.70 (45%) 5.50 (55%)	1.3×10^9	0.92
	>10	0	1.03 (15%) 8.50 (85%)	8.6×10^8	0.88
2:C_{60}	0	0	0.44 (47%) 6.03 (53%)	2.2×10^9	0.95
	1.0	0	0.91 (17%) 8.40 (83%)	9.9×10^8	0.90
	1.0	>10	0.65 (27%) 8.80 (73%)	1.4×10^9	0.93
	>10	0	1.50 (15%) 8.90 (85%)	5.6×10^8	0.83
3:C_{60}	0	0	0.49 (25%) 7.70 (75%)	1.9×10^9	0.95
	1.0	0	0.92 (10%) 7.65 (90%)	9.8×10^8	0.90
	1.0	>10	0.66 (18%) 7.50 (82%)	1.4×10^9	0.93
	>10	0	1.10 (9%) 7.90 (91%)	8.0×10^8	0.88

On the other hand, recovery of the fluorescence quenching rates was observed when potassium cations were added to the supramolecular complex of the crown ether appended free-base porphyrin−fullerene, as shown in curve iii in Figure 6, suggesting that the insertion of the potassium ions into the crown ether voids destabilizes the supramolecular complex (Scheme 1b). As listed in Table 5, the fractions of the fast fluorescence decay part decreased with the potassium ion addition more than 1.0 mM; the $(\tau_f)_{complex}$ values also became long, recovering up to 80% of the initial value of porphyrin in the absence of added fullerene. In the supramolecular complex, the nonplanar crown ether interaction with C_{60} could not fully capture the potassium ions to release C_{60}.

Representative transient absorption spectra observed for **2:C_{60}** in the presence of potassium ions are shown in Figure 9. Under these solution conditions, the intensity of the C_{60} anion radical at 1080 nm was weak compared with the triplet state absorption bands of C_{60} and H_2P as predominant peaks. However, the time profile of the absorption monitored at 1080 nm showed a slow rise in addition to a weak quick rise decay. The slow rise is typical of that expected for intermolecular electron transfer via the triplet excited states of C_{60} and H_2P,[26] whereas a weak quick rise decay can be attributed to the intramolecular charge-separation and charge-recombination processes of the complex remaining even by the addition of the potassium ions. The rate of the $C_{60}^{\bullet-}$ growth was found to increase with increasing C_{60} concentration indicating the occurrence of a bimolecular electron-transfer process. The bimolecular rate constant evaluated from the spectral data was found to be 3.25×10^{10} M^{-1} s^{-1} for **2** (with K^+) and **C_{60}**. Under the present experimental conditions, this process can be solely attributed to the intermolecular electron transfer from H_2P to $^3C_{60}$* (or from ^3H_2P* to C_{60}). The bimolecular rate constants for all of the studied systems ($(1.8-3.0) \times 10^{10}$ M^{-1} s^{-1}) were found to be slightly higher than the diffusion-controlled limit calculated in benzonitrile ($k_{diff} \sim 5.0 \times 10^9$ M^{-1} s^{-1}). These results clearly demonstrate potassium ion controlled switching of intramolecular electron transfer via the singlet excited porphyrin to intermolecular electron transfer from the triplet excited porphyrin in the studied systems.

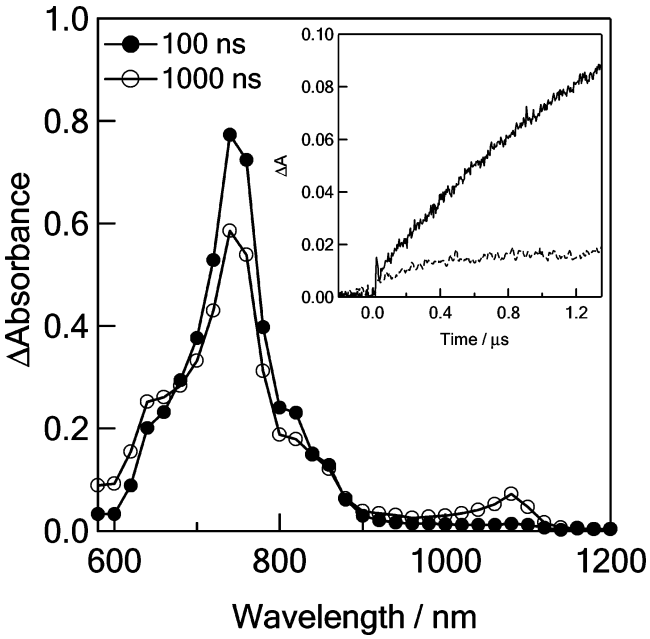

Figure 9. Nanosecond transient absorption spectra of **2** (0.10 mM) upon further addition of potassium ions (0.15 mM) in the presence of C_{60} (0.40 mM), after the 532 nm laser irradiation in benzonitrile. The figure inset shows the time profile of the fullerene anion radicals monitored at 1080 nm for **2** addition of potassium ion in the presence of **C_{60}** at 1:1 (dashed line) and 1:4 (solid line) ratios of **2:C_{60}**.

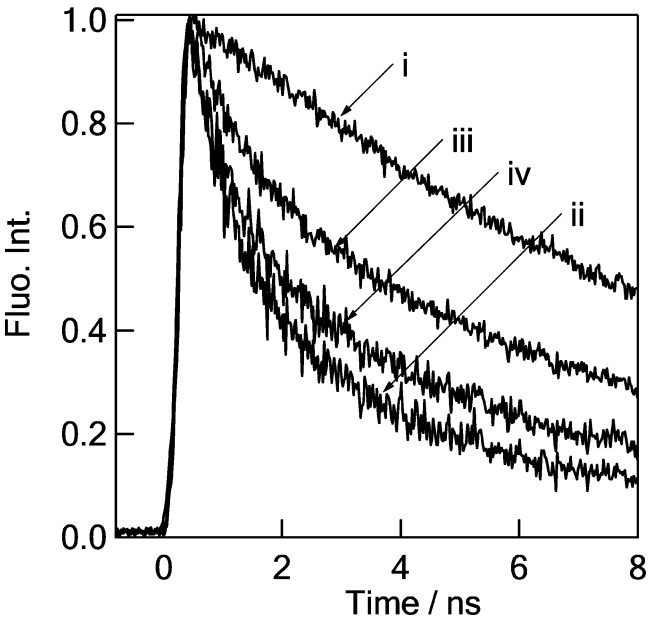

Figure 10. Fluorescence decays for (i) **1** (0.1 mM), (ii) **1** (0.1 mM) + **C_{60}** (0.1 mM), (iii) **1** (0.1 mM) + **C_{60}** (0.1 mM) + K^+ (1.0 mM), and (iv) **1** (0.1 mM) + **C_{60}** (0.1 mM) + K^+ (1.0 mM) + 18-crown-6 ether (>10.0 mM).

Inter- to Intramolecular Switching of Electron Transfer by Eliminating Potassium Ions from the Crown Ether Voids of the Supramolecular Complex. To switch the electron-transfer pathway inter- to intramolecular (Scheme 1b, backward reaction), the potassium ions captured in the cavity of the crown ether appended free-base porphyrin in the supramolecular dyad with C_{60} were extracted by the addition of excess 18-crown-6 ether. As shown in the fluorescence time profiles in Figure 10, the addition of 18-crown-6 ether (curve iv) reaccelerated the

recovered fluorescence decay in the presence of the potassium ions to supramolecular dyad (curve iii), although not completely to overlap on curve ii. This observation indicates that the addition of excess 18-crown-6 ether eliminates most of the potassium ions in the cavity of crown ether appended free-base porphyrin in the supramolecular dyad with C_{60} and changes the electron-transfer path inter- to intramolecular. That is, successful switching of the electron-transfer path of the supramolecular dyads by the insertion and the elimination of potassium ions was accomplished in the present study.

Summary

Several interesting observations were made from the results of the present study. The crown ether appended free-base porphyrins formed moderately stable complexes with C_{60} in which the binding constants were found to depend on the location and number of crown ether entities on the porphyrin ring and the utilized solvent media. Increasing the number of crown ether entities increased the binding constant of the resulting dyad. Molecular modeling of the dyads using the B3LYP/3-21G(*) method revealed stable structures from which the deduced geometric parameters revealed intramolecular interactions involving both porphyrin π-ring and crown ether entity(ies) with the fullerene in a cooperative fashion. A charge-transfer interaction as one of the mechanisms of supramolecular complex formation was evidenced from the molecular potential energy maps. The experimentally determined free-energy change for electron transfer (ΔG_{CS}), calculated by using the data from electrochemistry, fluorescence emission, and molecular modeling, suggested that electron transfer from singlet excited free-base porphyrin to C_{60} is energetically favorable in these dyads. Consequently, the photochemical studies probed by using picosecond time-resolved emission and nanosecond transient absorption techniques revealed intra−supramolecular light induced electron transfer from the singlet excited free-base porphyrin to the bound C_{60}. The measured k_{CS} values tracked the polarity of the solvents. In general, the calculated k_{CS} and Φ_{CS} revealed efficient charge separation, and the k_{CR} revealed charge stabilization to some extent in these dyads.

Interestingly, the addition of potassium ions to the donor−acceptor complex, the crown ether moiety(ies) of the porphyrins, destabilized the intramolecular interactions. Under these solutions conditions, intermolecular electron transfer was mainly observed. The measured bimolecular electron-transfer rate constants were close to that estimated for the diffusion-controlled process. Interestingly, switching of an inter- to intramolecular electron-transfer path was achieved by extracting the complexed potassium ions by the external addition of 18-crown-6 to the solution. Collectively, the present results nicely demonstrate the utilization of supramolecular principles (i) to obtain stable self-assembled donor−acceptor dyads to achieve efficient charge separation and (ii) switching of the photochemical electron-transfer pathway from intra- to intermolecular by complexing K^+ to the crown ether appended free-base porphyrins and inter- to intramolecular by further addition of 18-crown-6 to extract the bound K^+ from the crown ether appended free-base porphyrin.

Experimental Section

Chemicals. Fullerene, C_{60}, was from SES Research, Houston, TX. The syntheses and characterization of the crown ether appended free-base porphyrins are given elsewhere[17b] and were freshly purified over silica gel column prior to the spectral studies. All the chromatographic materials and solvents were procured from Fisher Scientific and were used as received. Tetra-*n*-butylammonium perchlorate, $(n\text{-}C_4H_9)_4NClO_4$, was from Fluka Chemicals. All other chemicals utilized in the synthesis and studies were from Aldrich Chemicals (Milwaukee, WI) and were used as received.

Instrumentation. The UV−vis spectral measurements were carried out with a Shimadzu Model 1600 UV-vis spectrophotometer. The fluorescence emission was monitored by using a Spex Fluorolog-tau spectrometer. The right angle method was utilized. Cyclic voltammograms were recorded on an EG&G Model 263A potentiostat using a three electrode system. A glassy carbon electrode was used as the working electrode. A platinum wire served as the counter electrode, and a Ag/AgCl was used as the reference electrode. A ferrocene/ferrocenium redox couple was used as an internal standard. All the solutions were purged prior to electrochemical and spectral measurements using argon gas. The computational calculations were performed by DFT B3LYP/3-21G(*) methods with the GAUSSIAN 03 software package[22] on high-speed computers. The electrostatic potential maps were generated using the *GaussView* program.

Time-resolved Emission and Transient Absorption Measurements. The picosecond time-resolved fluorescence spectra were measured using an argon-ion pumped Ti:sapphire laser (Tsunami, pulse width = 2 ps) and a streak scope (Hamamatsu Photonics, response time = 10 ps). The details of the experimental setup are described elsewhere.[27] Nanosecond transient absorption spectra in the NIR region were measured by means of laser-flash photolysis; 532 nm light from a Nd:YAG laser (pulse width = 6 ns) was used as the exciting source and a Ge-avalanche-photodiode module was used for detecting the monitoring light from a pulsed Xe lamp as described in our previous report.[27]

Acknowledgment. The authors are thankful to the National Science Foundation (Grant 0453464 to F.D.), the donors of the Petroleum Research Fund administered by the American Chemical Society, and Grants-in-Aid for Scientific Research on Primary Area (417) from the Ministry of Education, Science, Sport and Culture of Japan (to O.I. and Y.A.).

Supporting Information Available: Absorbance and steady-state fluorescence spectra, fluorescence lifetimes, and transient absorption spectra. This material is available free of charge via the Internet at http://pubs.acs.org.

References and Notes

(1) (a) Sutin, N.; Brunschwig, B. S. *Adv. Chem. Ser.* **1990**, *226*, 65. (b) Sykes, A. G. *Chem. Br.* **1988**, *24*, 551. (c) Bertrand, P. *Biochimie* **1986**, *68*, 619. (d) Dreyer, J. L. *Experientia* **1984**, *40*, 653. (e) Bolton, J. R.; Mataga, N.; McLendon, G. *Adv. Chem. Ser.* **1991**, *228*, 295. (f) Sigel, H., Sigel, A., Eds. *Metal Ions in Biological Systems, Electron Transfer Reactions in Metalloproteins*; Marcel Dekker: New York, 1991; Vol. 27, p 537. (g) Wheeler, R. A. *Introduction to the Molecular Bioenergetics of Electron, Proton, and Energy Transfer*; ACS Symposium Series: American Chemical Society, Washington, DC, 2004; Vol. 883, p 1. (h) Leibl, W.; Mathis, P. *Electron Transfer in Photosynthesis*; Series on Photoconversion of Solar Energy: 2004; Vol. 2, p 117. (i) Rodgers, K. R.; Lukat-Rodgers, G. S. *Compr. Coord. Chem. II*, **2004**, *8*, 17.

(2) (a) Balzani, V.; Scandola, F. *Supramolecular Chemistry*; Ellis Horwood: New York, 1991. (b) Schlicke, B.; De Cola, L.; Belser, P.; Balzani, V. *Coord. Chem. Rev.* **2000**, *208*, 267. (c) De Silva, A. P.; Gunaratne, H. Q. N.; Gunnlaugsson, T.; Huxley, A. J. M.; Mccoy, C. P.; Rademacher, J. T.; Rice, T. E. *Adv. Supramol. Chem.* **1997**, *4*, 1. (d) Ashton, P. R.; Ballardini, R.; Balzani, V.; Credi, A.; Dress, K. R.; Ishow, E.; Kleverlaan, C. J.; Kocian, O.; Preece, J. A.; Spencer, N.; Stoddart, J. F.; Venturi, M.; Wenger, S. *Chem.−Eur. J.* **2000**, *6*, 3558. (e) For an overview of molecular electronics see, for instance: Molecular Electronics: Science

and Technology. Aviram, A.; Ratner, M., Eds.; *Ann. N. Y. Acad. Sci*. **1998**, *852* and references therein.

(3) (a) *Supramolecular Chemistry*; Atwood, J. L., Davies, J. E. D., MacNicol, D. D., Vögtle, F., Reinhoudt, D. N., Eds.; Pergamon: Oxford, U.K., 1996; Vol. 10, pp 171−185. (b) Dickert, F. L.; Haunschild, A. *Adv. Mater*. **1993**, *5*, 887. (c) Schierbaum, K. D.; Göpel, E. *Synth. Met*. **1993**, *61*, 37. (d) Dickert, F. L.; Bäumler, U. P. A.; Zwissler, G. K.; *Synth. Met*. **1993**, *61*, 47. (e) Schierbaum, K. D.; Weiss, T.; Thoden van Velzen, E. U.; Engbersen, J. F. J.; Reinhoudt, D. N. *Science* **1994**, *265*, 1413. (f) Bell, T. W.; Hext, N. M. *Chem. Soc. Rev*. **2004**, *33*, 589. (g) Sun, S.-S.; Lees, A. J. *Coord. Chem Rev*. **2002**, *230*, 171. (h) de Silva, A. P.; Gunaratne, H. Q. N.; Gunnlaugsson, T.; Huxley, A. J. M.; McCoy, C. P.; Rademacher, J. T.; Rice, T. E. *Chem. Rev*. **1997**, *97*, 1515. (i) Lehn, J. M. *Front. Supramol. Org. Chem. Photochem*. **1991**, 1−28. (j) Bell, T. W.; Hext, N. M. *Chem. Soc. Rev*. **2004**, *33*, 589.

(4) (a) Marcus, R. A.; Sutin, N. *Biochim. Biophys. Acta* **1985**, *811*, 265. (b) Marcus, R. A.; *Angew. Chem., Int. Ed. Engl*. **1993**, *32*, 1111. (c) Bixon, M.; Jortner, J. *Adv. Chem. Phys*. **1999**, *106*, 35.

(5) (a) Kirmaier, C.; Holton, D. In *The Photosynthetic Reaction Center*; Deisenhofer, J., Norris, J. R., Eds.; Academic Press: San Diego, CA, 1993; Vol. II, pp 49−70. (b) Balzani, V.; Juris, A.; Venturi, M.; Campagna, S.; Serroni, S. *Chem. Rev*. **1996**, *96*, 759.

(6) (a) Miller, J. R.; Calcaterra, L. T.; Closs, G. L. *J. Am. Chem. Soc*. **1984**, *106*, 3047. (b) Closs, G. L.; Miller, J. R. *Science* **1988**, *240*, 440. (c) Connolly, J. S.; Bolton, J. R. In *Photoinduced Electron Transfer*; Fox, M. A., Chanon, M., Eds.; Elsevier: Amsterdam, The Netherlands, 1988; Part D, pp 303−393.

(7) (a) Wasielewski, M. R. *Chem. Rev*. **1992**, *92*, 435. (b) Kurreck, H.; Huber, M. *Angew. Chem., Int. Ed. Engl*. **1995**, *34*, 849. (c) Gust, D.; Moore, T. A.; Moore, A. L. *Acc. Chem. Res*. **2001**, *34*, 40.

(8) (a) Sessler, J. S.; Wang, B.; Springs, S. L.; Brown, C. T. In *Comprehensive Supramolecular Chemistry*; Atwood, J. L., Davies, J. E. D., MacNicol, D. D., Vögtle, F., Eds.; Pergamon: New York, 1996; Chapter 9. (b) Hayashi, T.; Ogoshi, H. *Chem. Soc. Rev*. **1997**, *26*, 355. (c) Ward, M. W. *Chem. Soc. Rev*. **1997**, *26*, 365.

(9) (a) Gust D.; Moore, T. A. In *The Porphyrin Handbook*; Kadish, K. M., Smith, K. M., Guilard, R., Eds.; Academic Press: Burlington, MA, 2000; Vol. 8, pp 153−190. (b) Imahori, H.; Sakata, Y. *Adv. Mater*. **1997**, *9*, 537. (c) Prato, M. *J. Mater. Chem*. **1997**, *7*, 1097. (d) Martín, N.; Sánchez, L.; Illescas, B.; Pérez, I. *Chem. Rev*. **1998**, *98*, 2527. (e) Diederich, F.; Gómez-López, M. *Chem. Soc. Rev*. **1999**, *28*, 263.

(10) (a) Guldi, D. M. *Chem. Commun*. **2000**, 321. (b) Guldi, D. M.; Prato, M. *Acc. Chem. Res*. **2000**, *33*, 695. (c) Guldi, D. M. *Chem. Soc. Rev*. **2002**, *31*, 22. (d) Meijer, M. E.; van Klink, G. P. M.; van Koten, G. *Coord. Chem. Rev*. **2002**, *230*, 141. (e) El-Khouly, M. E.; Ito, O.; Smith, P. M.; D'Souza, F. *J. Photochem. Photobiol., C* **2004**, *5*, 79. (f) Imahori, H.; Fukuzumi, S. *Adv. Funct. Mater*. **2004**, *14*, 525. (g) D'Souza, F.; Ito, O. *Coord. Chem. Rev*. **2005**, *249*, 1410.

(11) (a) Imahori, H.; Yamada, K.; Hasegawa, M.; Taniguchi, S.; Okada, T.; Sakata, Y. *Angew. Chem., Int. Ed. Engl*. **1997**, *36*, 2626. (b) Luo, C.; Guldi, D. M.; Imahori, H.; Tamaki, K.; Sakata, Y. *J. Am. Chem. Soc*. **2000**, *122*, 6535. (c) Imahori; H.; Guldi; D. M.; Tamaki, K.; Yoshida; Y.; Luo, C.; Sakata; Y.; Fukuzumi, S. *J. Am. Chem. Soc*. **2001**, *123*, 6617. (d) Imahori, H.; Tamaki, K.; Araki, Y.; Sekiguchi, Y.; Ito, O.; Sakata, Y.; Fukuzumi, S. *J. Am. Chem. Soc*. **2002**, *124*, 5165. (e) Liddell, P. A.; Kodis, G.; Moore, A. L.; Moore, T. A.; Gust, D. *J. Am. Chem. Soc*. **2002**, *124*, 7668. (f) Watanabe, N.; Kihara, N.; Furusho, T.; Takata, T.; Araki, Y.; Ito, O. *Angew. Chem., Int. Ed*. **2003**, *42*, 681. (g) De la Torre, G.; Giacalone, F.; Segura, J. L.; Martin, N.; Guldi, D. M. *Chem.−Eur. J*. **2005**, *11*, 1267. (h) Georghiou, P. E.; Tran, A. H.; Mizyed, S.; Bancu, M.; Scott, L. T. *J. Org. Chem*. **2005**, *70*, 6158.

(12) (a) Tkachenko, N. V.; Rantala, L.; Tauber, A. Y.; Helaja, J.; Hynninen, P. H.; Lemmetyinen, H. *J. Am. Chem. Soc*. **1999**, *121*, 9378. (b) Kesti, T. J.; Tkachenko, N. V.; Vehmanen, V.; Yamada, H.; Imahori, H.; Fukuzumi, S.; Lemmetyinen, H. *J. Am. Chem. Soc*. **2002**, *124*, 8067. (c) Vehmanen, V.; Tkachenko, N. V.; Efimov, A.; Damlin, P.; Ivaska, A.; Lemmetyinen, H. *J. Phys. Chem. A* **2002**, *106*, 8029. (d) Tkachenko, N. V.; Lemmetyinen, H.; Sonoda, J.; Ohkubo, K.; Sato, K.; Imahori, H.; Fukuzumi, S. *J. Phys. Chem. A* **2003**, *107*, 8834. (e) Chukharev, V.; Tkachenko, N. V.; Efimov, A.; Guldi, D. M.; Hirsch, A.; Scheloske, M.; Lemmetyinen, H. *J. Phys. Chem. B* **2004**, *108*, 16377.

(13) (a) Imahori, H.; Hagiwara, K.; Aoki, M.; Akiyama, T.; Taniguchi, S.; Okada, T.; Shirakawa, M.; Sakata, Y. *J. Am. Chem. Soc*. **1996**, *118*, 11771. (b) Imahori, H.; Sakata, Y.; *Adv. Mater*. **1997**, *9*, 537. (c) Imahori, H.; Mori, Y.; Matano, Y. *Photochem. Photobiol., C* **2003**, *4*, 51. (d) Kuciauskas, D.; Lin, S.; Seely, G. R.; Moore, A. L.; Moore; T. A.; Gust, G.; Drovetskaya, T.; Reed, C. A.; Boyd, P. D. W. *J. Phys. Chem*. **1996**, *100*, 15926. (e) Gust, D.; Moore, T. A.; Moore, A. L. *Acc. Chem. Res*. **2001**, *34*, 40. (f) D'Souza, F.; Gadde, S.; Zandler, M. E.; Arkady, K.; El-Khouly, M. E.; Fujitsuka, M.; Ito, O. *J. Phys. Chem. A* **2002**, *106*, 12393. (g) D'Souza, F.; Deviprasad, G. R.; Zandler, M. E.; El-Khouly, M. E.; Fujitsuka, M.; Ito, O. *J. Phys. Chem. B* **2002**, *106*, 4952.

(14) (a) Olmstead, M. M.; Costa, D. A.; Maitra, K.; Noll, B. C.; Phillips, S. L.; Van Calcar, P. M.; Balch, A. L. *J. Am. Chem. Soc*. **1999**, *121*, 7090. (b) Boyd, P. D. W.; Hodgson, M. C.; Richard, C. E. F.; Oliver, A. G.; Chaker, L.; Brothers, P. J.; Bolskar, R. D.; Tham, F. S.; Reed, C. A. *J. Am. Chem. Soc*. **1999**, *121*, 10487. (c) Evans, D. R.; Fackler, N. L. P.; Xie, Z.; Rickard, C. E. F.; Boyd, P. D. W.; Reed, C. A. *J. Am. Chem. Soc*. **1999**, *121*, 8466. (d) Sun, Y.; Drovetskaya, T.; Bolskar, R. D.; Bau, R.; Boyd, P. D. W.; Reed, C. A. *J. Org. Chem*. **1997**, *62*, 3642. (e) Boyd, P. D. W.; Reed, C. A. *Acc. Chem. Res*. **2005**, *38*, 235. (f) Wang, Y.-B.; Lin, Z. *J. Am. Chem. Soc*. **2003**, *125*, 6072.

(15) (a) Dietel, E.; Hirsch, A.; Eicchorn, E.; Rieker, A.; Hackbarth, S.; Roder, B. *Chem. Commun*. **1998**, 1981. (b) Guldi, D. M.; Luo, C.; Prato, M.; Troisi, A.; Zerbetto, F.; Scheloske, M.; Dietel, E.; Bauer, E.; Hirsch, A. *J. Am. Chem. Soc*. **2001**, *123*, 9166. (c) Schuster, D. I.; Cheng, P.; Wilson, S. R.; Prokhorenko, V.; Katterle, M.; Holzwarth, A. R.; Braslavsky, S. E.; Klihm, G.; Williams, R. M.; Luo, C. *J. Am. Chem. Soc*. **1999**, *121*, 11599. (d) Solladié, N.; Walther, M. E.; Gross, M.; Duarte, T. M. F.; Bourgogne, C.; Nierengarten, J.-F. *Chem. Commun*. **2003**, 2412.

(16) (a) D'Souza, F.; Deviprasad, G. R.; El-Khouly, M. E.; Fujitsuka, M.; Ito, O. *J. Am. Chem. Soc*. **2001**, *123*, 5277. (b) D'Souza, F.; Deviprasad, G. R.; Zandler, M. E.; El-Khouly, M. E.; Fujitsuka, M.; Ito, O. *J. Phys. Chem. A* **2003**, *107*, 4801. (c) D'Souza, F.; Gadde, S.; Zandler, M. E.; Itou, M.; Araki, Y.; Ito, O. *Chem. Commun*. **2004**, 2276. (d) D'Souza, F.; Deviprasad, G. R.; Zandler, M. E.; Hoang, V. T.; Arkady, K.; Van Stipdonk, M.; Perera, A.; El-Khouly, M. E.; Fujitsuka, M.; Ito, O. *J. Phys. Chem. A* **2002**, *106*, 3243. (e) El-Khouly, M. E.; Rogers, L. M.; Zandler, M. E.; Suresh, G.; Fujitsuka, M.; Ito, O.; D'Souza, F. *ChemPhysChem* **2003**, *4*, 474. (f) D'Souza, F.; Smith, P. M.; Zandler, M. E.; McCarty, M. E.; Itou, M.; Araki, Y.; Ito, O. *J. Am. Chem. Soc*. **2004**, *126*, 7898.

(17) (a) D'Souza, F.; Chitta, R.; Gadde, S.; Zandler, M. E.; Sandanayaka, A. S. D.; Araki, Y.; Ito, O. *Chem. Commun*. **2005**, 1279. (b) D'Souza, F.; Chitta, R.; Gadde, S.; Zandler, M. E.; McCarty, A. L.; Sandanayaka, A. S. D.; Araki, Y.; Ito, O. *Chem.−Eur. J*. **2005**, *11*, 4416.

(18) (a) Imahori, H.; Hagiwara, K.; Akiyama, T.; Akoi, M.; Taniguchi, S.; Okada, S.; Shirakawa, M.; Sakata, Y. *Chem. Phys. Lett*. **1996**, *263*, 545. (b) Guldi, D. M.; Asmus, K. D. *J. Am. Chem. Soc*. **1997**, *119*, 5744. (c) Imahori, H.; El-Khouly, M. E.; Fujitsuka, M.; Ito, O.; Sakata, Y.; Fukuzumi, S. *J. Phys. Chem. A* **2001**, *105*, 325.

(19) (a) Lara, F.; Cruz, R.; Martinez, M.; Martinez, R.; Villaneda, B.; Ramirez, A.; Moreno, E.; Martinez, I.; Angeles, E. *Supramol. Chem*. **1999**, *10*, 185. (b) Saha, A.; Nayak, S. K.; Chottopadhyay, S.; Mukherjee, A. K. *J. Phys. Chem. B* **2003,** *107*, 11889. (c) Bhattacharya, S.; Sharma, A.; Nayak, S. K.; Chattopadhyay, S.; Mukherjee, A. K. *J. Phys. Chem*. **2003**, *107*, 4213. (d) Datta, K.; Banerjee, M.; Kukherjee, A. K. *J. Phys. Chem. B* **2004**, *108*, 16100.

(20) Luger, P.; Andre, C.; Rudert, R.; Zobel, D. *Acta Crystallogr. Sect. B: Struct. Sci*. **1992**, *48*, 33.

(21) Benesi, H. A.; Hildebrand, J. H. *J. Am. Chem. Soc*. **1949**, *71*, 2703.

(22) Frisch, M. J.; Trucks, G. W.; Schlegel, H. B.; Scuseria, G. E.; Robb, M. A.; Cheeseman, J. R.; Montgomery, J. A., Jr.; Vreven, T.; Kudin, K. N.; Burant, J. C.; Millam, J. M.; Iyengar, S. S.; Tomasi, J.; Barone, V.; Mennucci, B.; Cossi, M.; Scalmani, G.; Rega, N.; Petersson, G. A.; Nakatsuji, H.; Hada, M.; Ehara, M.; Toyota, K.; Fukuda, R.; Hasegawa, J.; Ishida, M.; Nakajima, T.; Honda, Y.; Kitao, O.; Nakai, H.; Klene, M.; Li, X.; Knox, J. E.; Hratchian, H. P.; Cross, J. B.; Bakken, V.; Adamo, C.; Jaramillo, J.; Gomperts, R.; Stratmann, R. E.; Yazyev, O.; Austin, A. J.; Cammi, R.; Pomelli, C.; Ochterski, J. W.; Ayala, P. Y.; Morokuma, K.; Voth, G. A.; Salvador, P.; Dannenberg, J. J.; Zakrzewski, V. G.; Dapprich, S.; Daniels, A. D.; Strain, M. C.; Farkas, O.; Malick, D. K.; Rabuck, A. D.; Raghavachari, K.; Foresman, J. B.; Ortiz, J. V.; Cui, Q.; Baboul, A. G.; Clifford, S.; Cioslowski, J.; Stefanov, B. B.; Liu, G.; Liashenko, A.; Piskorz, P.; Komaromi, I.; Martin, R. L.; Fox, D. J.; Keith, T.; Al-Laham, M. A.; Peng, C. Y.; Nanayakkara, A.; Challacombe, M.; Gill, P. M. W.; Johnson, B.; Chen, W.; Wong, M. W.; Gonzalez, C.; Pople, J. A. *Gaussian 03*, revision B-04; Gaussian, Inc.: Pittsburgh, PA, 2003.

(23) Chitta, R.; Rogers, L. M.; Wanklyn, A.; Karr, P. A.; Kahol, P. K.; Zandler, M. E.; D'Souza, F. *Inorg. Chem*. **2004**, *43*, 6969.

(24) (a) Rehm, D.; Weller, A. *Isr. J. Chem*. **1970**, *7*, 259. (b) Mataga, N.; Miyasaka, H. In *Electron Transfer*; Jortner, J., Bixon, M., Eds.; John Wiley & Sons: New York, 1999; Part 2, pp 431−496.

(25) (a) Matsumoto, K.; Fujitsuka, M.; Sato, T.; Onodera, S.; Ito, O. *J. Phys. Chem. B* **2000**, *104*, 11632. (b) Komamine, S.; Fujitsuka, M.; Ito, O.; Morikawa, K.; Miyata, K.; Ohno, T. *J. Phys. Chem. A* **2000**, *104*, 11497. (c) Yamazaki, M.; Araki, Y.; Fujitsuka, M.; Ito, O. *J. Phys. Chem. A* **2001**, *105*, 8615.

(26) (a) Nojiri, T.; Alam, M. M.; Konami, H.; Watanabe, A.; Ito, O. *J. Phys. Chem. A* **1997**, *101*, 7943. (b) El-Khouly, M. E.; Fujitsuka, M.; Ito, O. *J. Porphyrins Phthalocyanines* **2000**, *4*, 591.

(27) (a) Nojiri, T.; Watanabe, A.; Ito, O. *J. Phys. Chem. A* **1998**, *102*, 5215. (b) Ghosh, H. N.; Pal, H.; Sapre, A. V.; Mittal, J. P. *J. Am. Chem. Soc*. **1993**, *115*, 11722. (c) Fujitsuka, M.; Ito, O.; Yamashiro, T.; Aso, Y.; Otsubo, T. *J. Phys. Chem. A* **2000**, *104*, 4876.